

# The effect of the magnetic field profile on the plume and on the plasma flow in the Hall thruster

IEPC-2005-068

*Presented at the 29<sup>th</sup> International Electric Propulsion Conference, Princeton University  
October 31 – November 4, 2005*

A. Fruchtman\*

*Holon Academic Institute of Technology, 52 Golomb St., Holon 58102, Israel*

**Abstract:** Analyzing the unmagnetized ionization region in the Hall thruster, we demonstrate the decrease of the propellant utilization with the decrease of the mass flow rate. Increasing the length of the ionization region improves the propellant utilization up to some limit. The alternative way of increasing this utilization by increasing the intensity of the magnetic field in the ionization region is shown to be accompanied by an undesirable increase of the plume divergence. To prevent this divergence increase, a configuration in which the magnetic field reverses its direction at the boundary between the ionization and the acceleration regions is proposed. It is shown how to design the magnetic field so that the ionization layer is positioned where the magnetic field vanishes.

## Nomenclature

$m$	= atom mass
$v$	= ion flow velocity
$n$	= plasma density
$T$	= electron temperature
$v_e$	= electron flow velocity
$n_a$	= neutral-gas density
$v_a$	= neutral-gas flow velocity
$\sigma$	= ionization cross section
$\alpha_i \epsilon_i$	= ionization energy cost
$e$	= elementary charge
$\phi$	= electrostatic potential
$\dot{m}$	= propellant mass flow rate
$S$	= channel cross-section
$c$	= ion sound velocity
$M$	= Mach number
$L_{ion}$	= length of the ionization region
$\lambda_{ion}$	= ionization mean-free-path
$\nu_l$	= particle radial-loss frequency
$\eta_m$	= propellant utilization
$r_{out}, r_{in}$	= channel outer, inner radius

---

\*Professor, Sciences Department, fnfrucht@hait.ac.il.

## I. Introduction

Two of the main difficulties in the employment of Hall thrusters<sup>1</sup> for space propulsion are the decrease of the propellant utilization at low power and the large plume divergence. The low power Hall thruster usually operates with a lower mass flow rate of the propellant. We present a model that shows the decrease of propellant utilization in this case. Since the magnetic field is often weak near the anode, we model the plasma in the ionization region as unmagnetized. This modelling is presented in Sec. II. A way to increase the propellant utilization that is often considered, is to increase the ionizing-electrons residence time in the ionization region, by increasing the intensity of the magnetic field there. Employing our previous analysis,<sup>2</sup> we show that such an increase, achieved by flattening the profile of the magnetic field, should be accompanied by an increased plume divergence. To avoid this divergence increase, we propose a configuration in which the magnetic field reverses its direction at the boundary between the ionization and the acceleration regions. If the ionization layer is located where the magnetic field is zero, the plume divergence due to magnetic-field curvature should be minimal.<sup>2</sup> This analysis of the plume divergence due to magnetic-field curvature is presented in Sec. III. First experiments stimulated by this suggestion are presented in another paper in this conference.<sup>3</sup> In Sec. IV we present a modified version of our previous model of the flow in the Hall thruster,<sup>4</sup> which we use for designing a configuration such that the ionization layer is positioned at the minimum of the magnetic field intensity.

## II. The propellant utilization

We assume the magnetic field in the ionization region near the anode to be so weak that the electrons are unmagnetized. Momentum balance yields

$$m v^2 + n T = \text{const.} \quad (1)$$

Here  $m$ ,  $n$ , and  $v$  are the ion mass, density, and velocity, and  $T$  is the electron temperature. The continuity equation is

$$\frac{d}{dz}(n v) = \frac{d}{dz}(n v_e) = -\frac{d}{dz}(n_a v_a) = \beta n_a n - \nu_l n, \quad (2)$$

where  $\beta \equiv \langle \sigma v_f \rangle$ ,  $\sigma$  being the ionization cross-section and the notation  $\langle \rangle$  represents averaging over the distribution function of  $v_f$ , the electron velocity. Also,  $v_e$  is the electron flow velocity, and  $n_a$  and  $v_a$  are the density and flow velocity of the neutral gas. The last term on the right hand side (RHS) of the equation represents wall losses,  $\nu_l = 2c/(r_{out} - r_{in})$ , where  $c$  is the sound velocity and  $r_{out}$  and  $r_{in}$  the outer and inner channel radii. Combining the two equations we obtain:

$$\frac{(T - m v^2)}{\{1 - [dT/d \ln(nv)] / (m v^2 + T)\}} \frac{dv}{dz} = \beta n_a - \nu_l. \quad (3)$$

This equation has to be complemented with an energy equation:

$$\frac{d}{dz} \left[ n v_e \left( \frac{5}{2} T + \alpha_i \epsilon_i \right) \right] = e n v_e \frac{d\phi}{dz}, \quad (4)$$

where  $\alpha_i \epsilon_i$  is the energy cost for ionization,  $e$  the elementary charge, and  $\phi$  the electrostatic potential. Here we neglected the radial energy losses. Most of the potential drops across the acceleration region, while the current is large in the ionization region. We assume that most of the work by the electric field is done on the electrons in the acceleration region. We neglect the work of the electric field in the ionization region, omit the term on the RHS of Eq. 4, and write

$$n v_e \left( \frac{5}{2} T + \alpha_i \epsilon_i \right) = \text{const.} \quad (5)$$

An additional relation is

$$(n v + n_a v_a) S = \frac{\dot{m}}{m}, \quad (6)$$

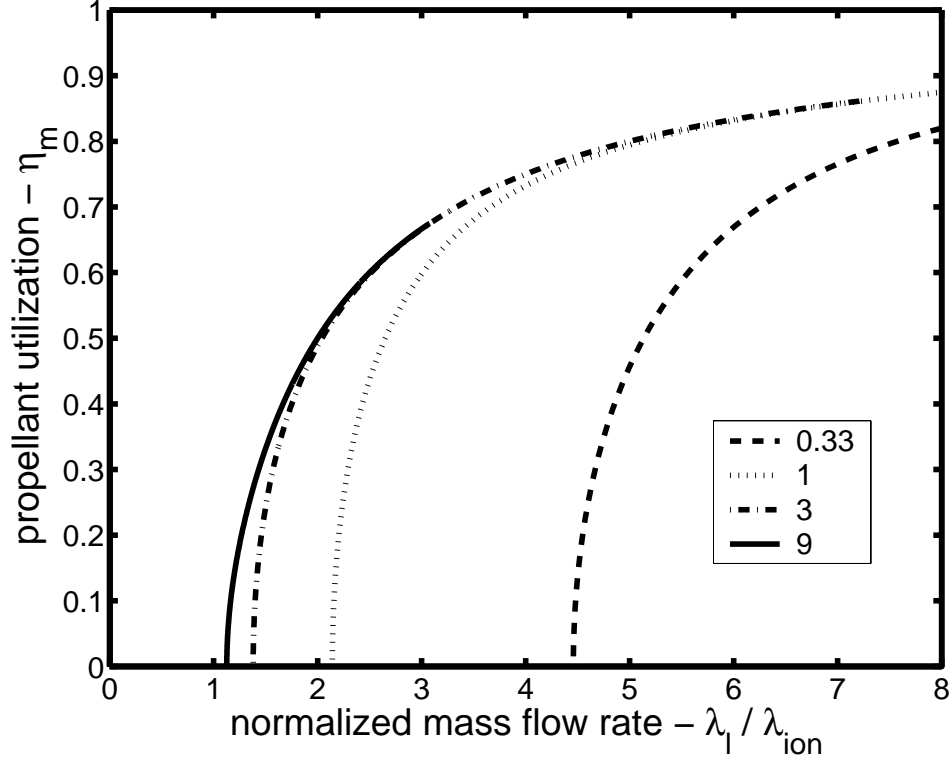


Figure 1. The propellant utilization as a function of normalized mass flow rate, for various values of the normalized length of the ionization region,  $L_{ion}/\lambda_l$ , which is also the ratio of the channel wall-area to channel cross-section.

where  $\dot{m}$  is the mass flow rate and  $S$  the channel cross-section. We assume that  $v_a$  is uniform in the channel and therefore Eq. (6) determines the value of the varying neutral density  $n_a$  along the channel as a function of the varying ion flux density  $nv$ . One final relation is for the discharge current density  $j_D = e(nv - nv_e)$ .

Although the decrease of the electron temperature along the ionization region is important in determining the ionization balance, we assume, for simplicity, that  $T$  is constant. The governing equation becomes

$$(1 - M^2) \frac{dM}{dz} = \frac{1}{\lambda_{ion}} \left(1 - \frac{\lambda_{ion}}{\lambda_l}\right) \left[ M^2 + 1 - \frac{2\eta_m}{(1 - \lambda_{ion}/\lambda_l)} M \right]. \quad (7)$$

Here  $c \equiv \sqrt{T/m}$ ,  $M \equiv v/c$ , and  $\eta_m \equiv (nv)_s Sm/\dot{m}$  is the propellant ionization. Here  $(nv)_s$  is the ion flux density at the thruster exit, assumed to be the same as at the sonic plane at the end of the ionization region. Also,  $\lambda_{ion} \equiv mSv_a c/\beta \dot{m}$  and  $\lambda_l \equiv c/\nu_l = (r_{out} - r_{in})/2$ . Solving the last equation, we obtain the profile of the velocity:

$$-M - \eta \ln(M^2 + 1 - 2\eta M) + 2\sqrt{1 - \eta^2} \left[ \arctan\left(\frac{M - \eta}{\sqrt{1 - \eta^2}}\right) - \arctan\left(\frac{-\eta}{\sqrt{1 - \eta^2}}\right) \right] = \frac{1}{\lambda_{ion}} \left(1 - \frac{\lambda_{ion}}{\lambda_l}\right) z. \quad (8)$$

Here  $\eta \equiv \eta_m/(1 - \lambda_{ion}/\lambda_l)$ .

we obtain a relation between the parameters by subtracting the values of the last equation for  $M = 1$  and  $M = -1$ .

$$-2 + \eta \ln\left(\frac{1 + \eta}{1 - \eta}\right) + 2\sqrt{1 - \eta^2} \left( \arctan\sqrt{\frac{1 - \eta}{1 + \eta}} + \arctan\sqrt{\frac{1 + \eta}{1 - \eta}} \right) = \frac{L_{ion}}{\lambda_l} \left( \frac{\lambda_l}{\lambda_{ion}} - 1 \right). \quad (9)$$

Assuming that the temperature  $T$  and the length of the ionization region  $L_{ion}$  are specified, we show in Fig. 1  $\eta_m$  as a function of the normalized mass flow rate  $\lambda_l/\lambda_{ion}$  for several values of  $L_{ion}/\lambda_l = 2L_{ion}/(r_{out} - r_{in})$ ,

the normalized length of the ionization region. The parameter  $L_{ion}/\lambda_l$  equals the ratio of the channel wall area to channel cross-section. These results explain the experimental findings,<sup>5</sup> that one can compensate for the decrease in propellant utilization due to a decrease of mass flow rate by increasing the channel length, and confirm the suggestion that wall losses could limit this compensation.<sup>5</sup> We note that in our model we have made the simplifying assumptions of specified electron temperature and length of the ionization region.

From the last relation we obtain a condition for plasma existence

$$\frac{L_{ion}}{\lambda_l} \left( \frac{\lambda_l}{\lambda_{ion}} - 1 \right) > \pi - 2 \quad \text{or} \quad \frac{L_{ion}}{\lambda_{ion}} - \frac{L_{ion}}{\lambda_l} > \pi - 2. \quad (10)$$

This shows that one can retain a high propellant utilization by increasing  $L_{ion}$  while  $\lambda_{ion}$  increases. However, the accompanying increase of  $L_{ion}/\lambda_l$  imposes a limit. A different way to avoid the decrease of the propellant utilization is to reduce electron mobility towards the anode by flattening the magnetic field profile so that the intensity of the magnetic field is increased there. Such a flattened magnetic field profile however, is expected to have an undesirable effect, an increase of the plume divergence. We discuss this effect on the plume divergence in the next section.

### III. Magnetic field curvature and plume divergence

The focusing effect of the magnetic field curvature on the plasma flow has been long recognized and configurations are designed in an attempt to take advantage of this effect.<sup>6-8</sup> In Ref. 2 we presented a simple analytical description of this focusing effect. We derived an expression for the radial (denoted as  $x$ ) velocity of the ions as they reach the cathode:

$$v_x = -\frac{m_e x_0 j_e}{m j_i} \int_{z_{peak}}^L \frac{\omega_{ce}^2}{\nu B_x} \frac{\partial B_x}{\partial z} dz. \quad (11)$$

In this expression, obtained within the paraxial approximation,  $x(z) = x_0$  is the approximately constant radial coordinate of the ions along their trajectory and  $z_{peak}$  is the location of the ionization layer. Also,  $B_x(z)$  is the intensity of the radial magnetic field,  $\nu$  the electron collisionality,  $\omega_{ce} \equiv eB_x/m_e$ ,  $m_e$  the electron mass,  $j_e \equiv -env_e$  and  $j_i \equiv env$  assumed constant in the acceleration region. Momentum balance, in which plasma thrust results from magnetic-field pressure, yields

$$v_0 = \frac{m_e}{m j_i} \int_{z_{peak}}^L j_e \frac{\omega_{ce}^2}{\nu} dz. \quad (12)$$

The divergence angle is therefore

$$\frac{v_x}{v_0} = -x_0 \frac{\int_{z_{peak}}^L (j_e \omega_{ce}^2 / \nu B_x) (\partial B_x / \partial z) dz}{\int_{z_{peak}}^L (j_e \omega_{ce}^2 / \nu) dz}. \quad (13)$$

We showed that when, as often it is assumed, the electron anomalous collisionality is  $\nu = \nu(B)$ , as in the case of Bohm diffusion, the last expression can be written as

$$\frac{v_x}{v_0} = -x_0 \frac{\int_{B_x(z_{peak})}^{B_x(L)} (\omega_{ce}^2 / \nu B_x) dB_x}{\int_{z_{peak}}^L (\omega_{ce}^2 / \nu) dz}. \quad (14)$$

The net effect is *divergence*, if ions are born in the magnetized region while the cathode is localized outside the magnetized region,  $B_x(L) = 0$ .

Incidentally, if we assume further that the Hall parameter  $\omega_{ce}/\nu$  is constant, the divergence angle becomes:

$$\frac{v_x}{v_0} = \frac{a(B_i - B_f)}{(A_f - A_i)} = \frac{aB_i}{L\bar{B}}. \quad (15)$$

Here  $\bar{B}$  is the average value of the magnetic field,  $B_i$  and  $B_f$  and  $A_i$  and  $A_f$  are values of the magnetic field and of the vector potential at the beginning and at the end of the acceleration channel,  $a$  is half the distance between the inner and outer walls, and we assume that  $B_f = 0$ .

From the last equation it is clear that to the lowest order the plasma lens is symmetrical. Zero divergence angle is obtained if  $B_i = B_f$ . In particular, if the cathode is located outside of the magnetic field,  $B_x(L) = 0$ , the ionization layer should also be positioned outside the magnetic field at the anode side. However, this contradicts the need to have a nonzero magnetic field near the anode for ionization improvement. We propose, therefore, to employ a configuration in which the magnetic field reverses its direction near the anode and to force the ionization layer to be positioned at the zero of this cusp configuration. Such a configuration should help in both increasing the ionization and reducing the plume divergence.

Configurations in which the magnetic field reverses its direction have been investigated. The above analysis seems to explain certain observed improvement of performance.<sup>6,7</sup>

The question arises how to determine the position of the ionization layer for specified parameters of the Hall thruster. This is analyzed in the next section.

#### IV. The acceleration region

The structure of the flow in the Hall thruster includes an ionization layer, an acceleration region and a backflow region. This structure was first suggested in Ref. 9. A numerical description of the flow that exhibited this structure as well as various analytical relations between the parameters was first presented in a theoretical model by Ahedo *et al.*<sup>10</sup> We derived a model that enables one to determine analytically the flow structure in the regime of intense ionization at a narrow layer.<sup>4</sup> The existence of a backflow region and an anode sheath in certain conditions was recently questioned.<sup>11–13</sup> We restrict this analysis to the case that a backflow region does exist.

We use a simplified and somewhat modified version of our model.<sup>4</sup> In the acceleration region

$$\frac{5}{2}\alpha T = e\phi, \quad (16)$$

where  $\alpha$  is a parameter that expresses electron losses. Such a linear dependence of the temperature on the potential has been suggested theoretically in the past.<sup>14</sup> Although a modified dependence that results from secondary electron emission was also considered,<sup>15</sup> we use here this linear dependence of the temperature on the potential that also has been experimentally observed.<sup>16</sup> When the electron energy is only affected by the electric-field work,  $\alpha = 1$ . The electron temperature in the Hall thruster that was found to vary linearly with the potential<sup>16</sup> did not seem to follow Eq. (16) with  $\alpha = 1$ . Whether due to a certain amount of ionization<sup>17</sup> or to other reason, I assume the form (16), in which  $\alpha > 1$  expresses a certain amount of electron energy losses in the ionization region.

At the sonic transition (which is different from the isothermal case of Sec. II):

$$\frac{m_i v_s^2}{2} = \frac{5}{6} T_s, \quad (17)$$

and therefore

$$T_s = \frac{3}{10} \frac{e\phi_A}{(1/4 + 3\alpha/4)}. \quad (18)$$

Assuming an intense full ionization,<sup>10,4</sup> we write

$$n_s (m_i v_i^2 + T)_s = (nT)_{peak}, \quad (19)$$

and also  $n_s v_s = \dot{m}/Sm$ . We therefore obtain:

$$(nT)_{peak} = \frac{8}{5\sqrt{1+3\alpha}} \frac{\dot{m}}{S} v_0. \quad (20)$$

Momentum balance across the acceleration region yields:

$$\left(1 - \frac{8}{5\sqrt{1+3\alpha}}\right) \frac{\dot{m}}{S} v_0 = \frac{m_e}{e} j_{eC} \int_{z_{peak}}^L dz \nu_d. \quad (21)$$

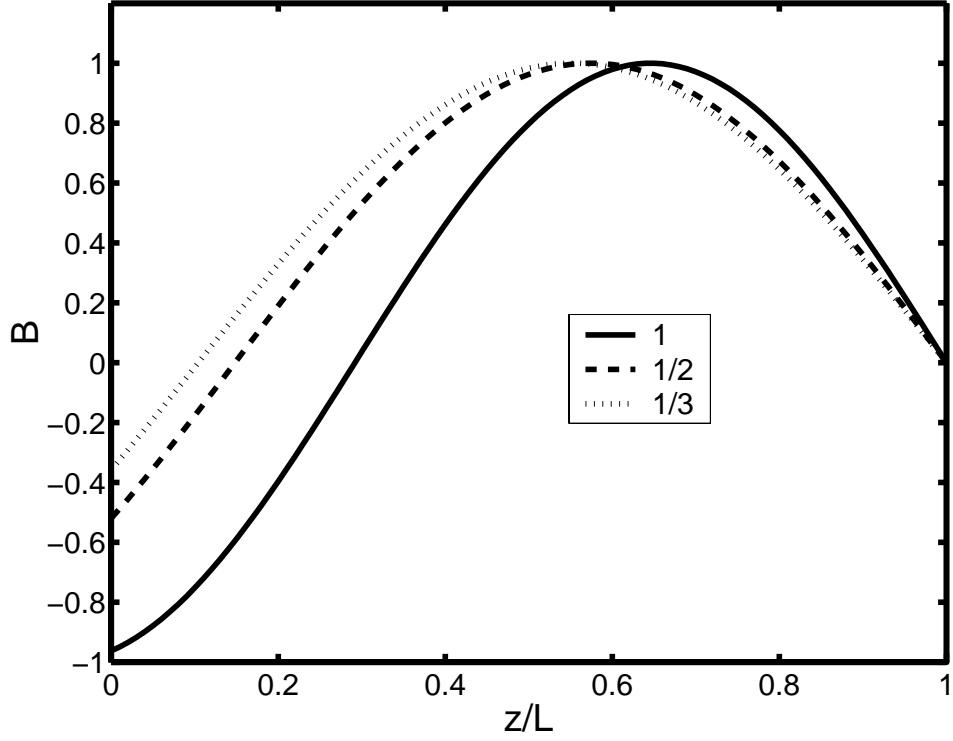


**Figure 2.** Reversing-direction magnetic-field profiles for various values of the maximal normalized electron temperature  $1/\alpha = 5T_{\max}/2e\phi_A$ , designed so that the ionization layer is positioned at the zero of the magnetic field.

Here  $\nu_d \equiv \omega_{ce}^2/\nu$  and  $j_{eC}$  is the constant electron current in the acceleration region. Similarly, through momentum balance across the *magnetized* backflow region, we obtain

$$\frac{8}{5\sqrt{1+3\alpha}} \frac{\dot{m}}{S} v_0 = \frac{m_e}{e} j_{eA} \int_0^{z_{peak}} dz \nu_d. \quad (22)$$

Here  $j_{eA}$  is the constant electron current in the backflow region. This picture of a substantial magnetic-field pressure across the thruster channel and a narrow current layer is different from the broad unmagnetized layer analyzed in Sec. II.

For the energy balance in the ionization region (ionizations layer and backflow region) we assume the same form as in Sec. II (5)

$$n v_e \left( \frac{5}{2} T + \alpha_i \epsilon_i \right) = -\frac{j_{eC}}{e} (\alpha \phi_A + \alpha_i \epsilon_i) = -\frac{j_{eA}}{e} \alpha_i \epsilon_i. \quad (23)$$

This simplified version of the more rigorous energy relations<sup>4</sup> is a reasonable approximation. From the last three relations we obtain

$$\int_0^{z_{peak}} dz \nu_d = \frac{1}{(5\sqrt{1+3\alpha}/8 - 1) \alpha e \phi_A / \alpha_i \epsilon_i + 5\sqrt{1+3\alpha}/8} \int_0^L dz \nu_d \quad (24)$$

This relation determines the location of the ionization layer. We assume anomalous electron collisionality such that  $\nu$  is proportional to  $\omega_{ce}$ . Then  $\nu_d$  is proportional to  $|B|$ .

We show how we design a thruster with a cusp configuration so that the ionization layer be located at the plane (in the 1D picture) of zero magnetic field. We assume a magnetic field of the form:

$$B_x = -B_0 \sin \left[ (\pi + p) \left( \frac{z}{L} - 1 \right) \right], \quad (25)$$

where for a cusp configuration  $0 \leq p \leq \pi/2$ . The magnetic field reverses its direction at  $z_0/L = p/(\pi + p)$ . In order that  $z_0 = z_{peak}$  we require that

$$\frac{1 + \cos(\pi + p)}{3 + \cos(\pi + p)} = \frac{1}{(5\sqrt{1 + 3\alpha}/8 - 1) \alpha e\phi_A / \alpha_i \epsilon_i + 5\sqrt{1 + 3\alpha}/8}. \quad (26)$$

Figure 2 shows the magnetic field profiles calculated from the last equation for three different values of  $1/\alpha$ . The value of  $\alpha$  determines the maximal electron temperature in the channel through  $T_{max}/e\phi_A = 2/(5\alpha)$ . The last relation determines the value of  $p$  and therefore the presented magnetic-field profile. In the calculation we assumed  $\alpha_i \epsilon_i / e\phi_A = 0.1$ .

## Acknowledgments

The author is grateful to Y. Raitses and to J. Ashkenazy for useful comments. This research has been partially supported by Israel Ministry of Industry (through Rafael) and by the Israel Science Foundation (Grant 59/99).

## References

- <sup>1</sup>Morozov, A. I., Esipchuk, Yu. V., Tilinin, G. N., Trofinov, A. V., Sharov, Yu. A., and Shahepkin, G. Ya., *Soviet Physics Technical Physics*, Vol. 17, 1972, p. 38.
- <sup>2</sup>Fruchtman, A. and Cohen-Zur, A., "Plume Divergence in the Hall Thruster," AIAA Paper 2004-3957, *40<sup>th</sup> Joint Propulsion Conference*, Fort Lauderdale, FL, July 11-14, 2004.
- <sup>3</sup>Ashkenazy, J., Shitrit, S., and Appelbaum G., Paper IEPC-2005-080, *29<sup>th</sup> International Electric Propulsion Conference*, Princeton University, October 31<sup>st</sup> - November 4<sup>th</sup>, 2005.
- <sup>4</sup>Cohen - Zur, A., Fruchtman, A., Ashkenazy, J., and Gany, A., "Analysis of the Steady-State Axial Flow in the Hall Thruster," *Physics of Plasmas*, Vol. 9, 2002, p. 4363.
- <sup>5</sup>Ashkenazy, J., Raitses, Y., and Appelbaum, G., "Parametric Studies of the Hall Current Plasma Thruster," *Physics of Plasmas* Vol. 5, 1998, p. 2055.
- <sup>6</sup>Hofer, R. R., Peterson, Y. P., and Gallimore, A. D., "A High Specific Impulse Two-Stage Hall Thruster with Plasma Lens Focusing," Paper IEPC-01-036, *27<sup>th</sup> International Electric Propulsion Conference*, Pasadena, CA, 15-19 October, 2001.
- <sup>7</sup>Hofer, R. R., and Gallimore, A. D., "The Role of Magnetic Field Topography in Improving the Performance of High-Voltage Hall Thrusters," AIAA Paper 2002-4111, *38<sup>th</sup> Joint Propulsion Conference*, Indianapolis, Indiana, July 7-10, 2002.
- <sup>8</sup>M. Keidar and I. D. Boyd, "On the Magnetic Mirror Effect in Hall Thrusters," *Applied Physics Letters*, Vol. 87, 121501, 2005, pp. 1, 3.
- <sup>9</sup>Bishaev, A., and Kim, V., *Soviet Physics Technical Physics*, Vol. 23, 1978, p.1055; Kim, V., *Journal of Propulsion and Power*, Vol. 14, 1998, p.736.
- <sup>10</sup>Ahedo, E., Martinez-Cerezo, P., and Martinez-Sanchez, M., *Physics of Plasmas*, Vol. 8, 2001, p. 3058.
- <sup>11</sup>Dorf, L., Semenov, V., and Raitses, Y., "Anode Sheath in Hall Thrusters," *Applied Physics Letters*, Vol. 83, 200, pp. 2551, 2553.
- <sup>12</sup>Dorf, L., Raitses, Y., Fisch, N. J., and Semenov, V., "Effect of Anode Dielectric Coating on Hall Thruster Operation," *Applied Physics Letters*, Vol. 84, 2004, pp. 1070, 1072.
- <sup>13</sup>Ahedo, E. and Rus, J., "Vanishing of the Negative Anode Sheath in a Hall Thruster," *Journal of Applied Physics*, Vol. 98, 043306, 2005, pp. 1, 7.
- <sup>14</sup>Zharinov, A. and Y. S. Popov, Y. S., *Soviet Physics Technical Physics*, Vol. 12, 1967, p. 208.
- <sup>15</sup>Choueiri, E. Y., "Fundamental Differences between Two Variants of Hall Thruster," *Physics of Plasmas*, Vol. 8, 2001, pp. 5025, 5033.
- <sup>16</sup>Staack, D., Raitses, Y., and Fisch, N. J., "Temperature Gradient in Hall Thrusters," *Applied Physics Letters*, Vol. 84, 2004, pp. 3028, 3030.
- <sup>17</sup>Cappelli, M., private communication (2004).